

Supplementary material to Numerical modeling and observations of seismo-acoustic waves propagating as modes in a fluid-solid waveguide

Jean Lecoulant^{1, 1, [a](#)} Claude Guennou,¹ Laurent Guillon,² and Jean-Yves Royer¹

¹*Laboratoire Géosciences Océan, Institut Universitaire Européen de la Mer,
Technopôle Brest-Iroise, Rue Dumont D'Urville, 29280 Plouzané,
France*

²*Institut de Recherche de l'École Navale, IRENav, BCRM de Brest,
École navale, CC 600 - Lanvéoc, F-29240 Brest Cedex 9,
France*

^ajean.lecoulant@univ-brest.fr

I. NUMERICAL MODELING

The modes propagating acoustic waves simulated 1500 m below the sea surface, with no intrinsic attenuation in the homogeneous crust (Configuration 1) and a source with a dominant frequency of 10 Hz are in good agreement with theoretical modes between 20 and 25 Hz (Fig 1).

The pressure simulated 400 km away from the source and 1500 m below the sea surface with intrinsic attenuation in a three-layered crust and a source with a dominant frequency of 1 Hz is almost identical in a 3000 m-deep homogeneous ocean (Configuration 3) and in a 3000 m-deep ocean with a SOFAR channel (Configuration 4a) (Fig. 2).

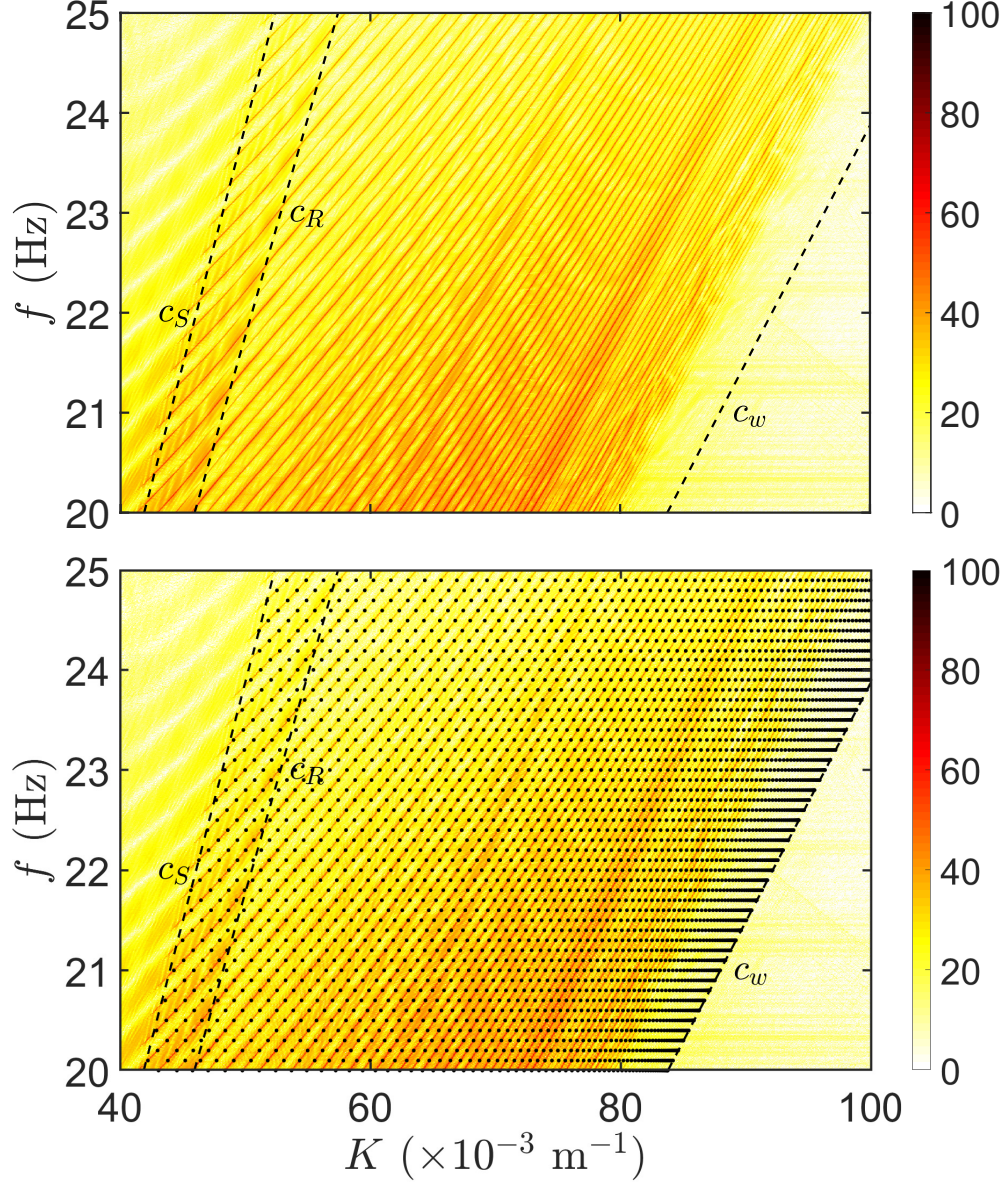


FIG. 1. (Color online) (Top) Frequency-wavenumber diagram of the normalized acoustic pressure showing the dispersion curves of simulated acoustic waves 1500 m below the sea surface, with no intrinsic attenuation in the homogeneous crust (Configuration 1) and a source with a dominant frequency of 10 Hz (colormap) between 20 and 25 Hz. Black dashed lines show the phase speed of sound in water (c_w), Rayleigh waves (c_R) and S waves (c_S). (Bottom) Same figure showing the theoretical modes (black dotted curves) matching the dispersion curves of simulated acoustic waves.

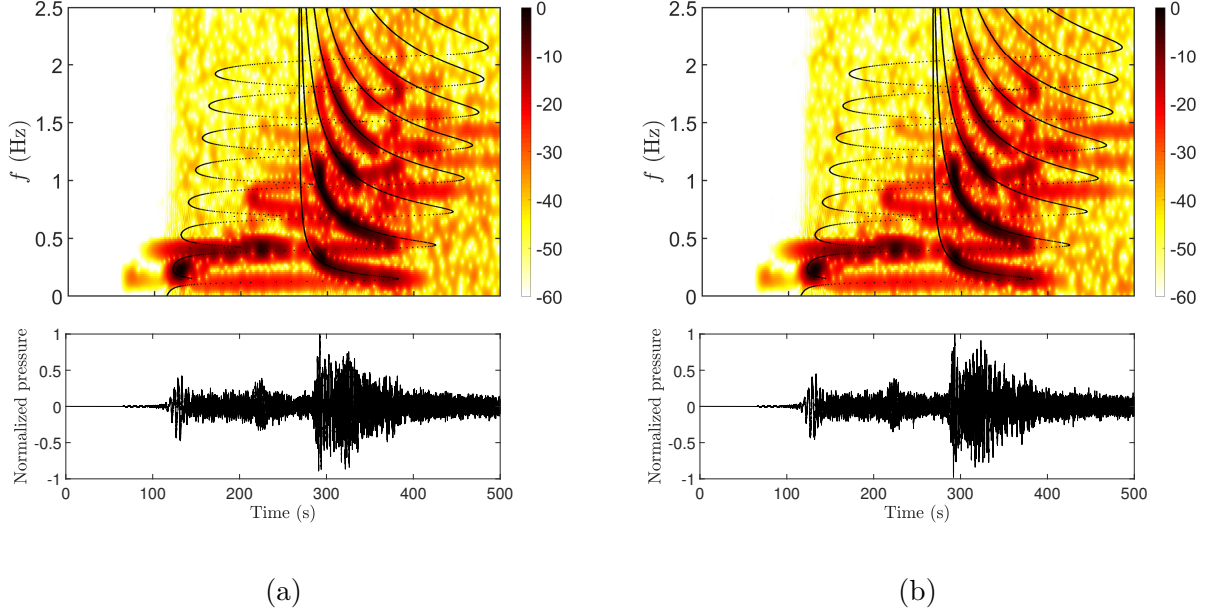


FIG. 2. (Color online) Spectrograms (top) and waveforms (bottom) of the pressure, 400 km away from the source and 1500 m below the sea surface with intrinsic attenuation in a three-layered crust, a source with a dominant frequency of 1 Hz, and a 3000 m-deep homogeneous ocean (Configuration 3) (a) or a 3000 m-deep ocean with a SOFAR channel (Configuration 4a) (b).

II. REAL CASE

The waves generated in the crust and in the ocean by the March 15, 2013 earthquake are visible on the vertical component of six ocean bottom seismometers (OBS) from the SWIR array, in the RHUM-RUM network. All waveforms show three successive arrivals that can be interpreted as P waves, interface waves and T waves (Fig. 3). The arrival times of P waves and interface waves are listed in Table I. Combined with the distances between the OBSs and the epicenter, these arrival times give the mean speeds of P waves (c_P^{eff}) and of interface waves (c_R^{eff}), which are then used to deduce the mean speeds of S waves (c_S^{eff}) by inverting numerically the approximation of the speed of Rayleigh waves by Viktorov (1967).

19 The theoretical arrival times of modes are calculated for each OBS using its distance to
 20 the epicenter, the local depth, and c_P^{eff} and c_S^{eff} (Tab. I) and are superimposed on the
 21 spectrograms (Fig. 3). All spectrograms show interface waves arriving as two modes with a
 22 shape similar to the theoretical modes. The results at the stations RR47, RR44 and RR43
 23 are similar to the results discussed in details for station RR48: the theoretical mode 1 is in
 24 good agreement with the observed mode 1, while there is an offset in frequency for mode 0.
 25 At station RR46, the theoretical frequency of the mode 1 is higher than the observed one
 26 and at station RR41, the theoretical frequency of the mode 1 is lower than the observed
 27 one.

TABLE I. Physical parameters used to calculate the arrival times of theoretical modes shown in
 Figure 3.

Station	Depth (m)	Distance to epicenter (km)	Arrival time of P waves (s)	Arrival time of interface waves (s)	c_P^{eff} (m.s ⁻¹)	c_R^{eff} (m.s ⁻¹)	c_S^{eff} (m.s ⁻¹)
RR48	4830	511	69.4	133.4	7362	3830	4151
RR47	4582	533	77.1	139.9	6905	3807	4165
RR46	3640	552	80.1	143.6	6888	3844	4216
RR44	4548	532	72.4	137.1	7347	3879	4213
RR43	4264	543	77.6	148.1	7000	3668	3979
RR41	5430	573	82.1	151.9	6972	3773	4113

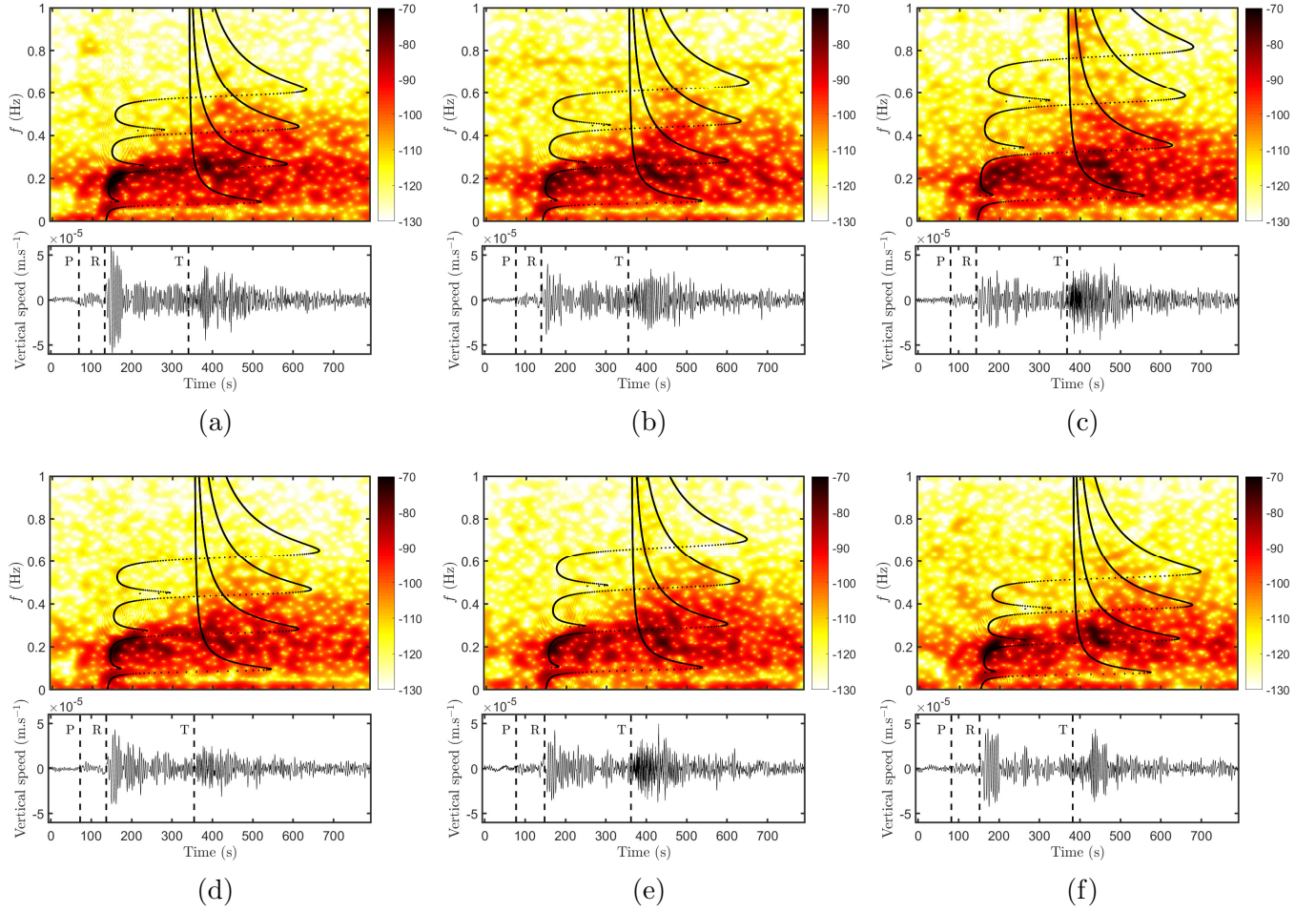


FIG. 3. (Color online) Spectrograms (top) with the predicted arrival times of theoretical modes according to the frequency (black dots) and waveforms high-pass filtered at 0.01 Hz (bottom) of the vertical component of OBSs RR48 (a), RR47 (b), RR46 (c), RR44 (d), RR43 (e) and RR41 (f). The dash lines annotated by the capital letters show the arrivals of P waves (P), precursory waves with a speed equal to c_R (R) and T waves (T), at times given in Table I.

¹Also at Institut de Recherche de l'École Navale, IRENav, BCRM de Brest, École navale, CC 600 - Lanvéoc,

F-29240 Brest Cedex 9, France

- ³¹ Viktorov, I. A. (1967). *Rayleigh and Lamb Waves Physical Theory and Applications*. Springer
- ³² US.